J. Condensed Matter Nucl. Sci. 39 (2025) 140–164

Research Article

Relativistic Phonon-Nuclear Coupling Matrix Element for the $D_2/^4He$ Transition

Peter L. Hagelstein

Massachusetts Institute of Technology, Cambridge, MA, USA

Abstract

We have proposed models for excess heat, transmutation, and low-level nuclear particle emission in PdD_x based on coherent nuclear dynamics involving highly excited nuclei. One of the first steps in the dynamics involves excitation transfer from the $D_2/^4He$ transition to other transitions, which means that to develop quantitative predictions from the model we need to evaluate the associated coupling matrix element. Transitions can be mediated by condensed matter degrees of freedom through electric dipole and magnetic dipole interactions ($-\mathbf{d}\cdot\mathbf{E}$ and $-\boldsymbol{\mu}\cdot\mathbf{B}$), but we have found that the relativistic phonon-nuclear interaction ($\mathbf{a}\cdot c\mathbf{P}$) provides a stronger coupling. We have evaluated $\mathbf{a}$ matrix elements for the molecular D_2 ^3P state transition to the ^1S state of the ^4He nucleus making use of simple single configuration wave functions. The wave function construction in both cases involves fully antisymmetrized wave functions that include spin, isospin and spatial components. Since the $\mathbf{a}$ operator is a rank 1 tensor operator, non-zero matrix elements are found only for the molecular ^3P $J=1$ states, as transitions to the $J=0$ and $J=2$ molecular states are forbidden.
 ISSN 2227-3123

Keywords: $D_2/^4He$ transition, low-energy nuclear reactions, n/p branching ratio, relativistic phonon-nuclear interaction, theory.

1. Introduction

Years ago, we attempted to develop quantitative estimates for rates associated with LENR processes (in particular, directional x-ray emission) based on theoretical models that we were working that could be compared with experimental data, with the result that we were not successful. For the up-conversion effect we were interested in to occur in experiments where the samples used were relatively small, the coupling between the lattice and internal nuclear degrees of freedom would need to be orders of magnitude stronger than what was estimated for electric and magnetic dipole coupling. Electric dipole coupling is generally regarded as being the strongest low-order interaction that has enough range to be useful (the strong force interactions are of short range) between nuclei and other nuclei and electrons in the lattice. Consequently, it is hard to imagine that there might be some low-order interaction orders of magnitude stronger that had been missed over the past century.

Nevertheless, it seemed unlikely at the time that the models would ever connect in a meaningful way without an interaction that could couple many nuclei together which was much stronger than electric dipole coupling. This

 ISSN 2227-3123

provided the motivation to think outside of the box, and to consider new ways an interaction might come about. At the time, the only possibility seemed to be if there was a residual coupling that resulted from the separation of center of mass and relative degrees of freedom in the relativistic problem [1]. For nonrelativistic models, the separation between the center of mass and relative degrees of freedom is clean in the sense that there is no coupling at all. The relativistic problem in a Dirac formalism does not separate cleanly. This should have led to some mixing of the center of mass and relative degrees of freedom, but there was no discussion of it in textbooks, or in papers we were familiar with. In the literature this issue seemed to be avoided [2], perhaps due in part to the absence of any experiments in which such a coupling was apparent.

In retrospect, such a coupling should be expected. A nucleus in motion undergoes changes due to relativity, which includes Lorentz contraction and internal spin rearrangement (such effects were studied in the case of the hydrogen atom in [3]). It is possible in principle to develop a description of the moving internal nucleus in terms of the rest frame internal states. Since the nucleus moves slowly in the lattice in response to vibrations and plasmons, the excited state admixture is expected to be small. Nevertheless, there must be an admixture, and this admixture has to change in response to changes in velocity associated with oscillations [1]. This argument provides for a physical basis for a relativistic phonon-nuclear interaction, in which the center of mass momentum (which is proportional to velocity in the lattice) is coupled to the internal nuclear degrees of freedom.

Once it was clear that we should expect there to be a coupling, then next issue is how to develop an appropriate mathematical description. On the one hand, relativistic quantum mechanics (Dirac models) provides a model that contains the effect [1], and which has the potential to yield an appropriate description of the interaction; however, this approach suffers from a lack of relativistic invariance, which means that we might worry that the interaction that results might be an artifact. This concern is amplified by the lack of consideration of the problem in the literature. On the other hand, the quantum field theories are relativistically invariant and capable of describing such an effect properly; however, it was not obvious initially how to extract such an interaction from a quantum field theory. To proceed, the idea was that it would be simplest to work with relativistic quantum mechanics to obtain the interaction, and then make use of field theory to confirm the result if possible.

In our early papers on the problem there was not much progress toward a workable theory that could be used to evaluate matrix elements systematically [4]. Eventually, we found the partial Foldy-Wouthuysen transformation, which provides an elegant tool with which the center of mass and relative degrees of freedom can be separated approximately within a multi-particle Dirac formalism. This leads to a scalar non-relativistic model for the center of mass, a relativistic Fermi-Kemmer-Yang type of description for the internal degrees of freedom, and clean low-order interaction terms that couple the center of mass and relative degrees of freedom [5]. Within the Dirac formalism, this looks to be the "right" approach to the problem.

The lowest-order interaction term found from this approach is

$$\hat{H}_{int} = \frac{1}{2Mc}\sum_{j<k}\left[\beta_j\boldsymbol{\alpha}_j + \beta_k\boldsymbol{\alpha}_k, \hat{V}_{jk}\right]\cdot c\mathbf{P} \tag{1}$$

where $[\cdots,\cdots]$ denotes the commutator, where $\hat{V}_{jk}$ is dominated by the nucleon-nucleon interaction, where M is the total mass, and where $\mathbf{P}$ is the center of mass momentum. The evaluation of matrix elements based on this formula is not particularly easy, primarily since it is a two-body operator. We worked on the reduction of this interaction, seeking results that could lead to a numerical evaluation for the coupling matrix element [6,7].

In the process of developing a paper on the interaction for the mainstream journals, we found that it was possible to reduce the matrix element from a complicated two-body interaction down to a much simpler single-particle interaction by making use of the identity [8]

$$\langle\Phi_1|[\hat{Q},\hat{H}]|\Phi_2\rangle = (E_2 - E_1)\langle\Phi_1|\hat{Q}|\Phi_2\rangle \tag{2}$$

After a reduction to a nonrelativistic formalism, the matrix element that results can be written as

$$\langle \Phi_1 | \hat{H}_{int} | \Phi_2 \rangle \;\rightarrow\; -i \frac{(E_2 - E_1)}{2Mc^2} \left\langle \Phi_1 \left| \sum_j \boldsymbol{\sigma}_j \times \frac{\boldsymbol{\pi}_j}{mc} \right| \Phi_2 \right\rangle \cdot c\mathbf{P} \tag{3}$$

where the $\boldsymbol{\sigma}_j$ operators are Pauli matrices, where the $\boldsymbol{\pi}_j$ are momentum variables associated with the relative degrees of freedom after separation from the center of mass degrees of freedom, and where m is the nucleon mass.

There remains the concern that this interaction is an artifact of the Dirac formalism, which is not relativistically invariant for realistic potentials. To address this, the partial Foldy-Wouthuysen transformation was applied to a two-body Bethe-Salpeter model (which is relativistically invariant), and a very similar interaction was found [8].

Now that we have the phonon nuclear matrix element in this form, we are motivated to make use of it for applications. The simplest application is the development of rough quantitative estimates for the magnitude of the matrix element, which is considered in Appendix A. From such simple quantitative estimates, it is clear that the coupling was weaker than some estimates that we had made earlier. We suggested that this might be due to an unknown symmetry in the system [8]; however, more likely this is due to our inexperience in developing quantitative estimates. Now that matrix elements of the lowest-order phonon-nuclear interaction can be evaluated in terms of one-body operators, we have the possibility of evaluating matrix elements for different systems of interest. In what follows we present a calculation of the phonon-nuclear interaction for the D_2/^{4}He transitions.

The relativistic coupling between the center of mass and relative degrees of freedom under consideration is extremely strong, orders of magnitude stronger than what might be expected from electric dipole coupling under comparable conditions. This is quantified in Appendix A. Since this interaction is so strong, it raises the question of why there are no earlier experiments (prior to experiments in LENR) where it was seen. One thought is that electromagnetic interactions are ubiquitous, so we are used to thinking about fundamental interactions showing up in all kinds of different experimental settings. However, this phonon nuclear coupling looks to be very specific – it would be most apparent if one were interested in Dicke-enhanced nuclear dynamics among excited states in a lattice, but in other problems it might not contribute anything significant.

One might expect an analog of the effect involving electrons bound to atoms that move. In this case we would make use of Equation (3) where the $\boldsymbol{\sigma}_j$ and $\boldsymbol{\pi}_j$ operators would apply to bound electrons (which are part of the composite atom), and where the nucleon mass m would then be replaced by the electron mass m_e. Presumably the interaction would provide for phonon coupling with inner shell electrons that move with the nucleus (and perhaps less so with electrons involved in bonds). It is not clear at this point under what conditions consequences of this interaction would important.

Since the interaction under consideration is not so familiar, it is reasonable to ask whether the $\boldsymbol{\sigma} \times \boldsymbol{\pi}$ operator has nice properties. Of particular importance is whether it transforms as a tensor operator (it would be disastrous if it didn't). A tensor operator behaves as we would expect intuitively, giving the same result if we rotated the coordinate system. Fortunately, the $\boldsymbol{\sigma} \times \boldsymbol{\pi}$ interaction transforms as a rank 1 tensor operator, as discussed in Appendix B. Because of this, matrix elements that are calculated must satisfy relations consistent with the Wigner-Eckart theorem, which can be used as a consistency check, and also to reduce the number of calculations that need to be done.

We are focused on the evaluation of the matrix element for the D_2/^{4}He transitions, in connection with claims of LENR anomalies in metal deuterides. Since molecular D_2 is a homonuclear diatomic molecule, the generalized Pauli principle [9] results in the elimination of about half of the states that might have been expected otherwise. If we focus on the nuclear spins, there can be ^{1}S and ^{5}S molecular states, ^{3}P states, and ^{1}D and ^{5}D states, etc. [10]. This means that we might expect electric dipole and magnetic dipole transitions starting from the ^{4}He ^{1}S ground state to be forbidden. In dd-fusion experiments that lead to gamma emission, electric and magnetic dipole transitions are observed [11]. This is a consequence of the small admixtures of LS coupled states with $J = 0$ to the ground state. The $\boldsymbol{\sigma} \times \boldsymbol{\pi}$ interaction is a magnetic quadrupole interaction, which means that there is allowed coupling to the ^{3}P states with $J = 1$. In our

construction, we evaluate coupling matrix elements to all of the ^{3}P states, but the coupling is finite only to the $J = 1$ states as expected.

Note that this selection rule has the potential for experimental consequences under conditions where the lowest-order interaction is dominant. For example, at low temperature it might be expected that D_2 molecules in the system might be predominantly in ^{1}S and ^{5}S states, so that the rate at which LENR D_2/^{4}He transitions occurs is reduced. At present we attribute low-level dd-fusion products to result from 3+1 fusion decay in connection with excitation transfer from the D_2/^{4}He transition to multiple Pd* excited states, which results in energetic p+t and n+^{3}He emission. If these transitions are mediated by the $\boldsymbol{\sigma} \times \boldsymbol{\pi}$ interaction, then we expect dd-fusion products to come from the ^{3}P $J = 1$ channel, for which the n/p branching ratio is about 0.93 based on the calculations in Tilley (1992). This is the opposite of the enhanced neutron yield observed in muon catalyzed fusion [12], where the yield from the $J = 1, \nu = 1$ μdd state is

$$R = \frac{Y(^3\mathrm{He} + n)}{Y(t + p)} = 1.455 \tag{4}$$

which is in good agreement with the $R = 1.43$ value predicted by Hale [13].

2. Coordinates and Spatial Wave Functions

Since the relativistic phonon-nuclear interaction under consideration in this paper couples the center of mass momentum to internal nuclear degrees of freedom, we need to develop a corresponding separation of the particle position and momentum operators. Since there are four particles, we will have one set of center of mass variables, and three sets of relative variables. The structure of the D_2 molecule suggests a natural set of coordinates for the relative degrees of freedom. It will be convenient to work with the internal relative coordinates between the two nucleons in each deuteron, as well as the separation between the two center of mass positions of the deuterons.

2.1. Coordinate Relations

We can define the center of mass coordinate and the internal molecular coordinates according to

$$\begin{gathered} \mathbf{R} = \frac{\mathbf{r}_1 + \mathbf{r}_2 + \mathbf{r}_3 + \mathbf{r}_4}{4} \\ \mathbf{r}_a = \mathbf{r}_2 - \mathbf{r}_1 \qquad\qquad \mathbf{r}_b = \mathbf{r}_4 - \mathbf{r}_3 \\ \mathbf{r} = \frac{\mathbf{r}_3 + \mathbf{r}_4}{2} - \frac{\mathbf{r}_1 + \mathbf{r}_2}{2} \end{gathered} \tag{5}$$

These are illustrated in Figure 1 for the 12;34 permutation (the overall wave function including spin and isospin must be antisymmetric under a permutation of any two particles).

2.2. Vector and Matrix Relations for Coordinates and Momenta

These relations and their inverse relations can be written in matrix form according to

$$\begin{pmatrix} \mathbf{R} \\ \mathbf{r}_a \\ \mathbf{r}_b \\ \mathbf{r} \end{pmatrix} = \mathbf{M} \cdot \begin{pmatrix} \mathbf{r}_1 \\ \mathbf{r}_2 \\ \mathbf{r}_3 \\ \mathbf{r}_4 \end{pmatrix} = \begin{pmatrix} \frac{1}{4} & \frac{1}{4} & \frac{1}{4} & \frac{1}{4} \\ -1 & 1 & 0 & 0 \\ 0 & 0 & -1 & 1 \\ -\frac{1}{2} & -\frac{1}{2} & \frac{1}{2} & \frac{1}{2} \end{pmatrix} \begin{pmatrix} \mathbf{r}_1 \\ \mathbf{r}_2 \\ \mathbf{r}_3 \\ \mathbf{r}_4 \end{pmatrix} \tag{6}$$

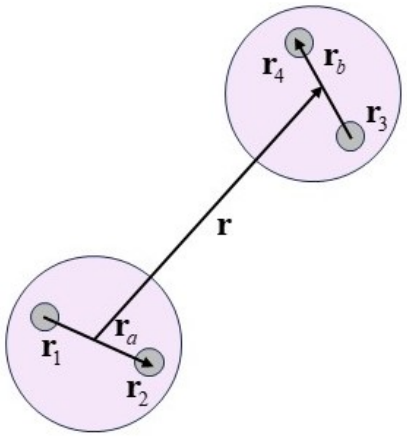

Figure 1. Internal coordinates for the D_2 molecule in the 12;34 permutation.

$$\begin{pmatrix} \mathbf{r}_1 \\ \mathbf{r}_2 \\ \mathbf{r}_3 \\ \mathbf{r}_4 \end{pmatrix} = \mathbf{M}^{-1} \cdot \begin{pmatrix} \mathbf{R} \\ \mathbf{r}_a \\ \mathbf{r}_b \\ \mathbf{r} \end{pmatrix} = \begin{pmatrix} 1 & -\frac{1}{2} & 0 & -\frac{1}{2} \\ 1 & \frac{1}{2} & 0 & -\frac{1}{2} \\ 1 & 0 & -\frac{1}{2} & \frac{1}{2} \\ 1 & 0 & \frac{1}{2} & \frac{1}{2} \end{pmatrix} \begin{pmatrix} \mathbf{R} \\ \mathbf{r}_a \\ \mathbf{r}_b \\ \mathbf{r} \end{pmatrix} \tag{7}$$

From these relations we can define corresponding relations between the momentum operators according to

$$\begin{pmatrix} \mathbf{p}_1 \\ \mathbf{p}_2 \\ \mathbf{p}_3 \\ \mathbf{p}_4 \end{pmatrix} = \mathbf{M}^{T} \cdot \begin{pmatrix} \mathbf{P} \\ \mathbf{p}_a \\ \mathbf{p}_b \\ \mathbf{p} \end{pmatrix} = \begin{pmatrix} \frac{1}{4} & -1 & 0 & -\frac{1}{2} \\ \frac{1}{4} & 1 & 0 & -\frac{1}{2} \\ \frac{1}{4} & 0 & -1 & \frac{1}{2} \\ \frac{1}{4} & 0 & 1 & \frac{1}{2} \end{pmatrix} \begin{pmatrix} \mathbf{P} \\ \mathbf{p}_a \\ \mathbf{p}_b \\ \mathbf{p} \end{pmatrix} \tag{8}$$

$$\begin{pmatrix} \mathbf{P} \\ \mathbf{p}_a \\ \mathbf{p}_b \\ \mathbf{p} \end{pmatrix} = (\mathbf{M}^{T})^{-1} \cdot \begin{pmatrix} \mathbf{p}_1 \\ \mathbf{p}_2 \\ \mathbf{p}_3 \\ \mathbf{p}_4 \end{pmatrix} = \begin{pmatrix} 1 & 1 & 1 & 1 \\ -\frac{1}{2} & \frac{1}{2} & 0 & 0 \\ 0 & 0 & -\frac{1}{2} & \frac{1}{2} \\ -\frac{1}{2} & -\frac{1}{2} & \frac{1}{2} & \frac{1}{2} \end{pmatrix} \begin{pmatrix} \mathbf{p}_1 \\ \mathbf{p}_2 \\ \mathbf{p}_3 \\ \mathbf{p}_4 \end{pmatrix} \tag{9}$$

2.3. Multidimensional Integration

Under this linear transformation of the coordinates, there is a corresponding modification of integrals according to

$$\begin{aligned} \int d^3\mathbf{r}_1 \int d^3\mathbf{r}_2 \int d^3\mathbf{r}_3 \int d^3\mathbf{r}_4 \Big\{ \cdots \Big\} &= \int d^3\mathbf{R} \int d^3\mathbf{r}_a \int d^3\mathbf{r}_b \int d^3\mathbf{r} |\det \mathbf{M}^{-1}| \Big\{ \cdots \Big\} \\ &= \int d^3\mathbf{R} \int d^3\mathbf{r}_a \int d^3\mathbf{r}_b \int d^3\mathbf{r} \Big\{ \cdots \Big\} \end{aligned} \tag{10}$$

where whatever function is being integrated on the LHS ($\{\cdots\}$) in terms of $\mathbf{r}_1 \cdots \mathbf{r}_4$ is also the same function in the integrals on the RHS, but with the coordinate transformation of Equation (7) implemented. The magnitude of the determinant of the Jacobian matrix $\mathbf{M}$ is unity.

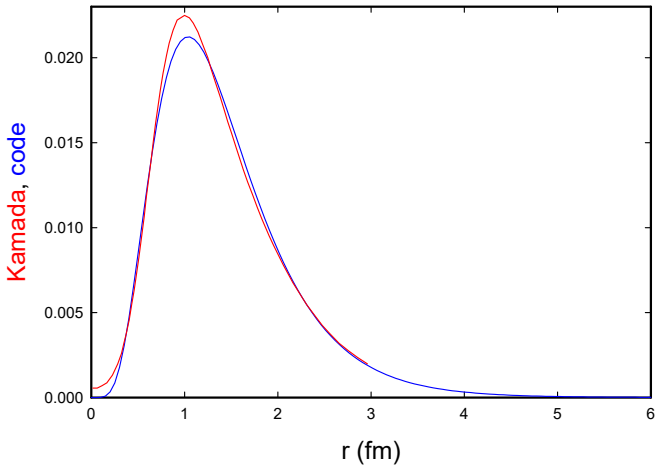

Figure 2. Comparison of the pair distribution function of Kamada et al (2001) and the pair distribution of our model wave function.

3. Spatial Parts of the ^{4}He and D_2 Wave Functions

For the spatial wave functions we follow the approach used previously in [4], but with improved wave functions.

3.1. ^{4}He Spatial Wave Function

In the model under consideration, the ^{4}He ground state spatial wave function will be taken to be

$$\Phi_S(\mathbf{r}_1,\mathbf{r}_2,\mathbf{r}_3,\mathbf{r}_4) = N_S\, u(|\mathbf{r}_2-\mathbf{r}_1|)u(|\mathbf{r}_3-\mathbf{r}_1|)u(|\mathbf{r}_4-\mathbf{r}_1|)u(|\mathbf{r}_3-\mathbf{r}_2|)u(|\mathbf{r}_4-\mathbf{r}_2|)u(|\mathbf{r}_4-\mathbf{r}_3|) \tag{11}$$

where N_S is a normalization factor. For the two-particle function u we have used

$$u(r) = (r-r_0)^t e^{-\alpha r^s} \tag{12}$$

with parameters

$$\begin{aligned} \alpha &= 7.092653899725\ \mathrm{fm}^{-s} \qquad s = 0.3330097498363 \\ t &= 2.151184405732 \qquad r_0 = 0.3003889154690\ \mathrm{fm} \end{aligned} \tag{13}$$

These parameters were optimized to produce a least squares best fit to the pair distribution function

$$C(|\mathbf{s}|) = \left\langle \delta(|\mathbf{s}| - |\mathbf{r}_{ij}|) \right\rangle \tag{14}$$

of Kamada et al. (2001) [14]. A comparison is shown in Figure 2.

Based on the coordinate transformations above, we normalize the spatial part of the wave function over relative coordinates according to

$$\int d^3\mathbf{r}_a \int d^3\mathbf{r}_b \int d^3\mathbf{r} \left\{ |\Phi_S|^2 \right\} = N_S^2 \int d^3\mathbf{r}_a \int d^3\mathbf{r}_b \int d^3\mathbf{r} \left\{ u(|\mathbf{r}_a|)u(|\mathbf{r}_b|) \right.$$
$$\left. u\left(\left|\mathbf{r} + \frac{\mathbf{r}_a - \mathbf{r}_b}{2}\right|\right) u\left(\left|\mathbf{r} + \frac{\mathbf{r}_a + \mathbf{r}_b}{2}\right|\right) u\left(\left|\mathbf{r} - \frac{\mathbf{r}_a + \mathbf{r}_b}{2}\right|\right) u\left(\left|\mathbf{r} + \frac{\mathbf{r}_b - \mathbf{r}_a}{2}\right|\right) \right\}^2$$

$$= N_S^2 8\pi^2 \int_0^\infty r^2 dr \int_0^\infty r^2 dr_a \int_0^\pi \sin\theta_a d\theta_a \int_0^\infty r^2 dr_b \int_0^\pi \sin\theta_b d\theta_b \int_0^{2\pi} d\phi_b \Bigg\{ u^2(r_a) u^2(r_b)$$
$$u^2\left(\sqrt{r^2 + \frac{r_a^2}{4} + \frac{r_b^2}{4} + r r_a \cos(\theta_a) + r r_b \cos(\theta_b) + \frac{r_a r_b}{2}\Big(\cos(\theta_a)\cos(\theta_b) + \sin(\theta_a)\sin(\theta_b)\cos(\phi_b)\Big)}\right)$$
$$u^2\left(\sqrt{r^2 + \frac{r_a^2}{4} + \frac{r_b^2}{4} + r r_a \cos(\theta_a) - r r_b \cos(\theta_b) - \frac{r_a r_b}{2}\Big(\cos(\theta_a)\cos(\theta_b) + \sin(\theta_a)\sin(\theta_b)\cos(\phi_b)\Big)}\right)$$
$$u^2\left(\sqrt{r^2 + \frac{r_a^2}{4} + \frac{r_b^2}{4} - r r_a \cos(\theta_a) + r r_b \cos(\theta_b) - \frac{r_a r_b}{2}\Big(\cos(\theta_a)\cos(\theta_b) + \sin(\theta_a)\sin(\theta_b)\cos(\phi_b)\Big)}\right)$$
$$u^2\left(\sqrt{r^2 + \frac{r_a^2}{4} + \frac{r_b^2}{4} - r r_a \cos(\theta_a) - r r_b \cos(\theta_b) + \frac{r_a r_b}{2}\Big(\cos(\theta_a)\cos(\theta_b) + \sin(\theta_a)\sin(\theta_b)\cos(\phi_b)\Big)}\right)\Bigg\}$$
$$= 1 \tag{15}$$

The mean square radius based on this model is

$$\sqrt{\langle |\mathbf{r}_4|^2 \rangle} = 1.448 \text{ fm} \tag{16}$$

which is a bit smaller than results from some of the wave functions considered in [16]. For the mean inter-nucleon separation we obtain

$$\sqrt{\langle |\mathbf{r}_{21}|^2 \rangle} = 2.364 \text{ fm} \tag{17}$$

which is also a bit smaller than values listed in [16].

3.2. Overall Molecular D_2 ^{3}P Spatial Wave Function

For the overall molecular D_2 ^{3}P spatial wave function we follow [4] and write for the 12;34 permutation (which corresponds to Figure 1)

$$\Phi_P(12;34) = \phi_d(|\mathbf{r}_2 - \mathbf{r}_1|)\phi_d(|\mathbf{r}_4 - \mathbf{r}_3|) R_{DD}\left(\left|\frac{\mathbf{r}_3 + \mathbf{r}_4}{2} - \frac{\mathbf{r}_1 + \mathbf{r}_2}{2}\right|\right) Y_{lm}(12;34) \tag{18}$$

where ϕ_d is the S part of the deuteron relative wave function, where R_{DD} is the radial wave function associated with the deuteron-deuteron separation, and where $Y(12;34)$ is the relevant spherical harmonic associated with the particular P state. A similar approach is discussed in [17] for deuteron-deuteron scattering.

3.3. Deuteron Spatial Wave Function

For the spatial part of the ^{3}S component of the deuteron wave function we developed a fit for the wave function published by Epelbaum (2005) [18], which is shown in Figure 3.

3.4. Molecular D_2 radial wave function

For the radial wave function of the D_2 molecule we solved the radial equation

$$E P_{DD}(r) = \left(-\frac{\hbar^2}{2\mu}\frac{d^2}{dr^2} + \frac{\hbar^2 l(l+1)}{2\mu r^2} + V_{mol}(r) + V_N^{S,l}(r)\right) P_{DD}(r) \tag{19}$$

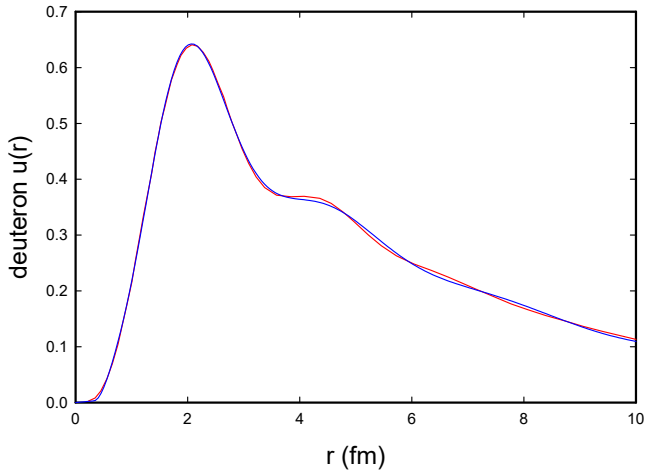

Figure 3. The ^{3}S component of the deuteron wave function based on the chiral effective field theory NNNLO interaction of Epelbaum (2005) (red); fitted version (blue).

where the nuclear potential is

$$V_N^{S,l}(r) = \frac{V_0}{1 + e^{(r-r_S)/a_S}} \tag{20}$$

with parameters for the ^{3}P channel taken to be [19]

$$V_0 = -13.5 \text{ MeV} \qquad r_S = 5.04 \text{ fm} \qquad a_S = 0.79 \text{ fm} \tag{21}$$

In the past we used the Frost-Musulin potential [20]. For this calculation we upgraded to the more accurate potential of Kolos and Wolniewicz (1986) [21], which we fit according to

$$V_{mol}(r) = \frac{e^2}{4\pi\epsilon_0 r}\left(1 - b_1\frac{r}{a_0} - b_2\frac{r^2}{a_0^2}\right)e^{-\alpha r^s} \tag{22}$$

with

$$\begin{aligned} \alpha &= 0.6255121237003474 \qquad & b_1 &= 1.47525721177208 \\ b_2 &= -0.2369829512108492 \qquad & s &= 1.065986412041894 \end{aligned} \tag{23}$$

From the normalized radial solution $P_{DD}(r)$ we fit according to

$$\frac{P_{DD}(r)}{r^2} = \frac{R_{DD}(r)}{r} = \sqrt{\frac{v_{nuc}}{v_{mol}}}e^{-G}F_{DD}(r) \tag{24}$$

with

$$F_{DD}(r) = \frac{b_0 + b_1 r + b_2 r^2 + b_3 r^3}{1 + c_1 r + c_2 r^2 + c_3 r^3} \tag{25}$$

where the fitting parameters (with r in fm) are

$$b_0 = -11.4896775161166 \qquad b_1 = 2.68207103102594$$

$$b_2 = -0.2214474891006211 \qquad b_3 = 0.0128023171027513$$
$$c_1 = -0.1856986934380801 \qquad c_2 = 0.0319483726096694 \qquad c_3 = 0.002875346842982812 \tag{26}$$

The idea here is that ultimately it is $F_{DD}(r)$ and $F'_{DD}(r)$ that appears in the integrals that we need to evaluate for the $\mathbf{a}$-matrix element, so it is appropriate that this should be what we focus on for the fit. For some years we have been working with matrix elements that are scaled according to

$$|\langle \Psi[\mathrm{D}_2]|\mathbf{a}|\Psi[^4\mathrm{He}]\rangle| \;\sim\; \sqrt{\frac{v_{nuc}}{v_{mol}}}e^{-G}(\cdots) \tag{27}$$

where v_{nuc} is a representative nuclear volume

$$v_{nuc} = \left(\frac{4\pi}{3}\ 5\ \mathrm{fm}\right)^3 \tag{28}$$

and where the molecular volume has been taken from earlier work to be

$$v_{mol} = \Big(2\pi R_0\Big)\Big(\pi(\Delta R)^2\Big) = 0.0788\ \mathring{\mathbf{A}}^3 \tag{29}$$

While reviewing the galley proof, we note that this is a poor approximation for the nuclear volume. For the ^{1}S and ^{5}S molecular states a better approximation would be

$$v_{mol} = 4\pi R_0^2 \Delta R = 0.508\ \mathring{\mathbf{A}}^3 \tag{30}$$

To correct this error would require changing many numbers throughout the paper. Since this molecular volume is used only as a scaling factor, and does not change the result obtained at the end, we have chosen to leave the numbers as calculated with the 0.0788 $\mathring{\mathrm{A}}^3$ molecular volume number.

The ratio evaluates to

$$\frac{v_{nuc}}{v_{mol}} = 6.64 \times 10^{-12} \tag{31}$$

The ratio used in [4] is slightly different, since the values for R_0 and ΔR that result from the solution of the radial wave function in the Frost-Musulin potential differ by a small amount from what we have used here

$$R_0 = 1.401080\ a_0 0 \qquad \Delta R = \sqrt{\frac{\hbar}{2\mu\omega_0}} \qquad \hbar\omega_0 = 0.3862729\ \mathrm{eV} \tag{32}$$

The Gamow factor used is based on the JWKB approximation (with no zero-point energy) for the ^{3}P channel

$$G = \int_{r_{min}}^{r_{max}} \sqrt{\frac{2\mu[V(r)-E]}{\hbar^2}}dr = 90.35 \tag{33}$$

4. Spin and Isospin Construction of the Wave Functions

For the numerical calculations we focus on the calculation of the matrix elements

$$\mathbf{M}(J, M_J; 0, 0) = \left\langle\ ^4\mathrm{He}\ J=0, M_J=0\middle|\sum_j \boldsymbol{\sigma}_j \times \boldsymbol{\pi}_j\middle|\mathrm{D}_2\ J, M_J\right\rangle \tag{34}$$

based on a reasonably simple model for the nuclear states. Since the transition is allowed, we should be able to develop a reasonable estimate based on wave functions for the deuterons and alpha particles in the absence of D-state admixtures. We recall that for the alpha particle, a complete description would involve a mix of ^{1}S, ^{3}P and ^{5}D components [22], [23].

Our goal is to construct a simple and easily understood model for the states, keeping in mind the need to work with fully antisymmetric wave functions. We have developed a construction of the states in a Mathematica script, which allows for a brute force reduction of the spin and isospin terms, as well as an integration over the angular variables. At the end of the Mathematica calculation, we end up with an analytic expression for the matrix element in terms of radial integrals that can be evaluated numerically.

4.1. Spin and Isospin Part of the ^{4}He Ground State Wave Function

Perhaps the simplest route to construct such a wave function is to start with a wave function that is not anti-symmetrized, but which is obviously in a spin singlet and isospin singlet state, and then anti-symmetrize it. We can write this as

$$\begin{aligned}
\Psi &= \mathcal{A}\Big\{ p\uparrow p\downarrow n\uparrow n\downarrow \Phi_S(\mathbf{r}_1,\mathbf{r}_2,\mathbf{r}_3,\mathbf{r}_4)\Big\} \\
&= \frac{1}{\sqrt{24}}\Big\{ p\uparrow p\downarrow n\uparrow n\downarrow - p\uparrow p\downarrow n\downarrow n\uparrow - p\uparrow n\uparrow p\downarrow n\downarrow \\
&\quad + p\uparrow n\downarrow p\downarrow n\uparrow + p\uparrow n\uparrow n\downarrow p\downarrow - p\uparrow n\downarrow n\uparrow p\downarrow \\
&\quad - p\downarrow p\uparrow n\uparrow n\downarrow + p\downarrow p\uparrow n\downarrow n\uparrow + n\uparrow p\uparrow p\downarrow n\downarrow \\
&\quad - n\downarrow p\uparrow p\downarrow n\uparrow - n\uparrow p\uparrow n\downarrow p\downarrow + n\downarrow p\uparrow n\uparrow p\downarrow \\
&\quad + p\downarrow n\uparrow p\uparrow n\downarrow - p\downarrow n\downarrow p\uparrow n\uparrow - n\uparrow p\downarrow p\uparrow n\downarrow \\
&\quad + n\downarrow p\downarrow p\uparrow n\uparrow + n\uparrow n\downarrow p\uparrow p\downarrow - n\downarrow n\uparrow p\uparrow p\downarrow \\
&\quad - p\downarrow n\uparrow n\downarrow p\uparrow + p\downarrow n\downarrow n\uparrow p\uparrow + n\uparrow p\downarrow n\downarrow p\uparrow \\
&\quad - n\downarrow p\downarrow n\uparrow p\uparrow - n\uparrow n\downarrow p\downarrow p\uparrow + n\downarrow n\uparrow p\downarrow p\uparrow \Big\}\Phi_S(\mathbf{r}_1,\mathbf{r}_2,\mathbf{r}_3,\mathbf{r}_4)
\end{aligned} \tag{35}$$

since the spatial part of the wave function Φ_S for the S state is fully symmetric upon the exchange of any two nucleons. We can get a sense of what the anti-symmetrization operator does in this result. All permutations of the nucleons in the different orbitals are generated, with a minus sign showing up every time two nucleons are switched. Since the spatial part of the wave function is invariant to nucleon exchange, it can be factored out. We make use of a short cut in the notation according to

$$p\uparrow p\downarrow n\uparrow n\downarrow \;\rightarrow\; |p\uparrow\rangle_1 \, |p\downarrow\rangle_2 \, |n\uparrow\rangle_3 \, |n\downarrow\rangle_4 \tag{36}$$

to keep track of the spin and isospin of the different nucleons. We can think of this wave function as being the product of a spatial part, and combined spin and isospin part according to

$$\Psi = \Big| T=0, S=0 \Big\rangle \Phi_S(\mathbf{r}_1,\mathbf{r}_2,\mathbf{r}_3,\mathbf{r}_4) \tag{37}$$

4.2. Spin and Isospin Part of the Molecular D_2 Wave Functions

We were motivated to attempt a similar group theory based construction for the molecular D_2 wave functions. This construction was hindered by errors that we noticed in the specification of the symmetric group Clebsch-Gordan

coefficients in the tables that we had available. The approach is very powerful, and in the future we hope that simple to understand and error-free tables become available. Perhaps there might be developed a Mathematica package which can evaluate the symmetric group Clebsch-Gordan coefficients in the future.

Instead, we started with a construction for the molecular D_2 wave functions that was simple, but not anti-symmetrized, based on

$$\begin{aligned}
\Psi(12;34|M_S=1) &= \Big|12;34|M_S=1\Big\rangle\Phi_P(12;34)\\
&= \Big|T=0,M_T=0\Big\rangle_{12}\Big|T=0,M_T=0\Big\rangle_{34}\Big|S=1,M_S=1\Big\rangle_{12;34}\Phi_P(12;34)\\
&= \left(\frac{p_1n_2-n_1p_2}{\sqrt{2}}\right)\left(\frac{p_3n_4-n_3p_4}{\sqrt{2}}\right)\left(\frac{\uparrow_1\uparrow_2\uparrow_3\downarrow_4+\uparrow_1\uparrow_2\downarrow_3\uparrow_4-\uparrow_1\downarrow_2\uparrow_3\uparrow_4-\downarrow_1\uparrow_2\uparrow_3\uparrow_4}{2}\right)\Phi_P(12;34)\\
&= \frac{1}{4}\Big(p\uparrow n\uparrow p\uparrow n\downarrow+p\uparrow n\uparrow p\downarrow n\uparrow-p\uparrow n\downarrow p\uparrow n\uparrow-p\downarrow n\uparrow p\uparrow n\uparrow\\
&\quad -p\uparrow n\uparrow n\uparrow p\downarrow-p\uparrow n\uparrow n\downarrow p\uparrow+p\uparrow n\downarrow n\uparrow p\uparrow+p\downarrow n\uparrow n\uparrow p\uparrow\\
&\quad -n\uparrow p\uparrow p\uparrow n\downarrow-n\uparrow p\uparrow p\downarrow n\uparrow+n\uparrow p\downarrow p\uparrow n\uparrow+n\downarrow p\uparrow p\uparrow n\uparrow\\
&\quad +n\uparrow p\uparrow n\uparrow p\downarrow+n\uparrow p\uparrow n\downarrow p\uparrow-n\uparrow p\downarrow n\uparrow p\uparrow-n\downarrow p\uparrow n\uparrow p\uparrow\Big)\Phi_P(12;34)
\end{aligned}\tag{38}$$

$$\begin{aligned}
\Psi(12;34|M_S=0) &= \Big|12;34|M_S=0\Big\rangle\Phi_P(12;34)\\
&= \Big|T=0,M_T=0\Big\rangle_{12}\Big|T=0,M_T=0\Big\rangle_{34}\Big|S=1,M_S=0\Big\rangle_{1234}\Phi_P(12;34)\\
&= \left(\frac{p_1n_2-n_1p_2}{\sqrt{2}}\right)\left(\frac{p_3n_4-n_3p_4}{\sqrt{2}}\right)\left(\frac{\uparrow\uparrow\downarrow\downarrow-\downarrow\downarrow\uparrow\uparrow}{\sqrt{2}}\right)\Phi_P(12;34)\\
&= \frac{1}{\sqrt{8}}\Big(p\uparrow n\uparrow p\downarrow n\downarrow-p\downarrow n\downarrow p\uparrow n\uparrow-p\uparrow n\uparrow n\downarrow p\downarrow+p\downarrow n\downarrow n\uparrow p\uparrow\\
&\quad -n\uparrow p\uparrow p\downarrow n\downarrow+n\downarrow p\downarrow p\uparrow n\uparrow+n\uparrow p\uparrow n\downarrow p\downarrow-n\downarrow p\downarrow n\uparrow p\uparrow\Big)\Phi_P(12;34)
\end{aligned}\tag{39}$$

$$\begin{aligned}
\Psi(12;34|M_S=-1) &= \Big|12;34|M_S=-1\Big\rangle\Phi_P(12;34)\\
&= \Big|T=0,M_T=0\Big\rangle_{12}\Big|T=0,M_T=0\Big\rangle_{34}\Big|S=1,M_S=-1\Big\rangle_{1234}\Phi_P(12;34)\\
&= \left(\frac{p_1n_2-n_1p_2}{\sqrt{2}}\right)\left(\frac{p_3n_4-n_3p_4}{\sqrt{2}}\right)\left(\frac{\uparrow_1\downarrow_2\downarrow_3\downarrow_4+\downarrow_1\uparrow_2\downarrow_3\downarrow_4-\downarrow_1\downarrow_2\uparrow_3\downarrow_4-\downarrow_1\downarrow_2\downarrow_3\uparrow_4}{2}\right)\Phi_P(12;34)\\
&= \frac{1}{4}\Big(p\uparrow n\downarrow p\downarrow n\downarrow+p\downarrow n\uparrow p\downarrow n\downarrow-p\downarrow n\downarrow p\uparrow n\downarrow-p\downarrow n\downarrow p\downarrow n\uparrow\\
&\quad -p\uparrow n\downarrow n\downarrow p\downarrow-p\downarrow n\uparrow n\downarrow p\downarrow+p\downarrow n\downarrow n\uparrow p\downarrow+p\downarrow n\downarrow n\downarrow p\uparrow\\
&\quad -n\uparrow p\downarrow p\downarrow n\downarrow-n\downarrow p\uparrow p\downarrow n\downarrow+n\downarrow p\downarrow p\uparrow n\downarrow+n\downarrow p\downarrow p\downarrow n\uparrow\\
&\quad +n\uparrow p\downarrow n\downarrow p\downarrow+n\downarrow p\uparrow n\downarrow p\downarrow-n\downarrow p\downarrow n\uparrow p\downarrow-n\downarrow p\downarrow n\downarrow p\uparrow\Big)\Phi_P(12;34)
\end{aligned}\tag{40}$$

Antisymmtrization of a two-deuteron wave function is discussed in [17]. These wave functions can be antisymmetrized according to

$$\mathcal{A}\Big\{\Psi(12;34|M_S)\Big\} = \frac{1}{\sqrt{6}}\Bigg(\Big|12;34|M_S\Big\rangle\Phi_P(12;34) - \Big|13;24|M_S\Big\rangle\Phi_P(13;24) - \Big|14;23|M_S\Big\rangle\Phi_P(14;23)$$

$$-\Big|23;14|M_S\Big\rangle\Phi_P(23;14) - \Big|24;13|M_S\Big\rangle\Phi_P(24;13) + \Big|34;12|M_S\Big\rangle\Phi_P(34;12)\Bigg) \tag{41}$$

The idea is that the different permutations can be obtained according to

$$\Big|13;24|M_S\Big\rangle = \hat{P}_{23}\Big|12;34|M_S\Big\rangle$$
$$\Phi_P(13;24) = -\hat{P}_{23}\Phi_P(12;34) \tag{42}$$

with analogous relations for the other cases.

This approach is the same as was used in [4], but with a different notation.

4.3. Construction of LSJ states

The construction outlined above results in LS states, which can be used to construct LSJ states. For this we use Clebsch-Gordan coefficients according to

$$|JM_J\rangle = \sum_m \sum_{M_S} |l,m\rangle|S,M_S\rangle\Big\langle l,m;S,M_s\Big|J,M_J\Big\rangle \tag{43}$$

5. Reduction of the Spin and Isospin Components

An advantage that comes with setting up the states in Mathematica script is that we can use Mathematica to reduce the spin and isospin parts of the matrix element, ultimately leading to spatial integrals. Selection rules that are expected emerge naturally in the course of the calculation. It is useful to focus first on the special case of a forbidden transition in order to understand better the results presented subsequently for the allowed transitions.

5.1. Matrix Element for the D_2 ^{3}P $J = 0$ State

We focus first on the molecular D_2 ^{3}P $J = 0$ state, where we expect the matrix element to vanish. For the spherical harmonics in the molecular D_2 wave function, we make use of

$$rY_{1,1} = -\sqrt{\frac{3}{4\pi}}\frac{x+iy}{\sqrt{2}} \qquad rY_{1,0} = \sqrt{\frac{3}{4\pi}}z \qquad rY_{1,-1} = \sqrt{\frac{3}{4\pi}}\frac{x-iy}{\sqrt{2}} \tag{44}$$

Based on a brute force Mathematica calculation, we obtain

$$\Big\langle\Psi[J=0,M_J=0]\Big|\sum_j \boldsymbol{\sigma}_j\times\boldsymbol{\pi}_j\Big|\Psi[^4\mathrm{He}]\Big\rangle = \frac{1}{\sqrt{288\pi}}\int d^3\mathbf{r}\int d^3\mathbf{r}_a\int d^3\mathbf{r}_b$$
$$\phi_d(12)\phi_d(34)F_{DD}(12;34)\Big\{-\hat{\mathbf{i}}_x\Big(y_1+y_2-y_3-y_4\Big)\Big((p_z)_1+(p_z)_2-(p_z)_3-(p_z)_4\Big)$$

$$
\begin{aligned}
&+\hat{\mathbf{i}}_x\Big(z_1+z_2-z_3-z_4\Big)\Big((p_y)_1+(p_y)_2-(p_y)_3-(p_y)_4\Big)\\
&+\hat{\mathbf{i}}_y\Big(x_1+x_2-x_3-x_4\Big)\Big((p_z)_1+(p_z)_2-(p_z)_3-(p_z)_4\Big)\\
&-\hat{\mathbf{i}}_y\Big(z_1+z_2-z_3-z_4\Big)\Big((p_x)_1+(p_x)_2-(p_x)_3-(p_x)_4\Big)\\
&-\hat{\mathbf{i}}_z\Big(x_1+x_2-x_3-x_4\Big)\Big((p_y)_1+(p_y)_2-(p_y)_3-(p_y)_4\Big)\\
&+\hat{\mathbf{i}}_z\Big(y_1+y_2-y_3-y_4\Big)\Big((p_x)_1+(p_x)_2-(p_x)_3-(p_x)_4\Big)\Big\}\Phi_S\\
&+\cdots
\end{aligned}
\tag{45}
$$

where the $\cdots$ indicate equivalent integrals associated with the five other permutations. Consequently, in this case we can take 6 times the result from the integrals in the first permutation and eliminate the other permutations (since they differ only by a renumbering). For this example we changed which wave functions are in which slot, in order to have the coordinates come before the momentum operators, to simplify the discussion.

We see that the spatial coordinates that appear are those of the separation between the two deuterons

$$\mathbf{r}=\frac{\mathbf{r}_3+\mathbf{r}_4}{2}-\frac{\mathbf{r}_1+\mathbf{r}_2}{2} \tag{46}$$

A similar observation follows for the appearance of the momentum operators (since our focus is on the relative problem, we can assume that $\mathbf{P}=0$ so that $\boldsymbol{\pi}_j=\mathbf{p}_j$ here).

For this matrix element, and for all of the others under consideration, the spin and isospin reduction results in position and momentum operators for the molecular D_2 relative degrees of freedom (there is no dependence on the deuteron coordinates $\mathbf{r}_a$ and $\mathbf{r}_b$ or their momenta).

Note that there is no angular momentum associated with the $\mathbf{r}$ degree of freedom in Φ_S or in F_{DD}, so that the matrix elements vanish. The conclusion is that there is no coupling from the ^{4}He ground state configuration to the molecular D_2 ^{3}P $J=0$ state, as expected for a rank 1 tensor operator.

5.2. Results for the $J=1$ Matrix Elements

Based on the discussion above, we can summarize the results from systematic Mathematica calculations for the spin and isospin reduction for all of the different matrix elements. We find that there is no coupling to the molecular D_2 ^{3}P $J=2$ states, again as expected. There is coupling to the D_2 ^{3}P $J=1$ states (also as expected). For the non-zero matrix elements we can write

$$
\begin{aligned}
\left\langle \Psi[^4\mathrm{He}]\middle|\sum_j \boldsymbol{\sigma}_j\times\boldsymbol{\pi}_j\middle|\Psi[J=1,M_J=+1]\right\rangle &= \sqrt{\frac{v_{nuc}}{v_{mol}}}e^{-G}\sqrt{\frac{3}{8\pi}}\int d^3\mathbf{r}\int d^3\mathbf{r}_a\int d^3\mathbf{r}_b\\
&\Big\{\Phi_S\phi_d(|\mathbf{r}_a|)\phi_d(|\mathbf{r}_b|)\Big[\hat{\mathbf{i}}_x\Big(ip_y y+ip_z z\Big)-\hat{\mathbf{i}}_y\Big(p_x x+p_z z\Big)\Big]F_{DD}(|\mathbf{r}|)\Big\}
\end{aligned}
\tag{47}
$$

$$
\begin{aligned}
\left\langle \Psi[^4\mathrm{He}]\middle|\sum_j \boldsymbol{\sigma}_j\times\boldsymbol{\pi}_j\middle|\Psi[J=1,M_J=0]\right\rangle &= \sqrt{\frac{v_{nuc}}{v_{mol}}}e^{-G}\sqrt{\frac{3}{4\pi}}\int d^3\mathbf{r}\int d^3\mathbf{r}_a\int d^3\mathbf{r}_b\\
&\Big\{\Phi_S\phi_d(|\mathbf{r}_a|)\phi_d(|\mathbf{r}_b|)\Big[-i\hat{\mathbf{i}}_z(p_x x+p_y y)\Big]F_{DD}(|\mathbf{r}|)\Big\}
\end{aligned}
\tag{48}
$$

$$\left\langle \Psi[^4\mathrm{He}] \middle| \sum_j \boldsymbol{\sigma}_j \times \boldsymbol{\pi}_j \middle| \Psi[J=1,M_J=-1] \right\rangle = \sqrt{\frac{v_{nuc}}{v_{mol}}} e^{-G} \sqrt{\frac{3}{8\pi}} \int d^3\mathbf{r} \int d^3\mathbf{r}_a \int d^3\mathbf{r}_b$$
$$\left\{ \Phi_S \phi_d(|\mathbf{r}_a|) \phi_d(|\mathbf{r}_b|) \left[-\hat{\mathbf{i}}_x \left(ip_y y + ip_z z \right) - \hat{\mathbf{i}}_y \left(p_x x + p_z z \right) \right] F_{DD}(|\mathbf{r}|) \right\} \tag{49}$$

5.3. Reduction for the $M_J = 0$ Matrix Element

Since the three matrix elements are related through the Wigner-Eckart theorem, we only need to evaluate one of them. The $M_J = 0$ matrix element is the simplest, so we focus on it. We can evaluate the derivatives associated with the momentum operators and obtain

$$\left\langle \Psi[^4\mathrm{He}] \middle| \sum_j \boldsymbol{\sigma}_j \times \boldsymbol{\pi}_j \middle| \Psi[J=1,M_J=0] \right\rangle = -\hat{\mathbf{i}}_z \hbar \sqrt{\frac{v_{nuc}}{v_{mol}}} e^{-G} \sqrt{\frac{3}{4\pi}} \int d^3\mathbf{r} \int d^3\mathbf{r}_a \int d^3\mathbf{r}_b$$
$$\left\{ \Phi_S(\mathbf{r},\mathbf{r}_a,\mathbf{r}_b) \phi_d(|\mathbf{r}_a|) \phi_d(|\mathbf{r}_b|) \left[\left(2F_{DD}(|\mathbf{r}|) + \frac{x^2+y^2}{r} F'_{DD}(|\mathbf{r}|) \right) \right] \right\} \tag{50}$$

where we have indicated the dependence of the ^{4}He nucleus spatial wave function. Since there is no dependence of the integrand on θ and ϕ other than $x^2 + y^2$, we can average according to

$$\frac{\int_0^\pi \sin\theta (x^2+y^2) d\theta}{\int_0^\pi \sin\theta d\theta} = r^2 \frac{\int_0^\pi \sin^3\theta d\theta}{\int_0^\pi \sin\theta d\theta} = \frac{4/3}{2} r^2 = \frac{2}{3} r^2 \tag{51}$$

This results in

$$\left\langle \Psi[^4\mathrm{He}] \middle| \sum_j \boldsymbol{\sigma}_j \times \boldsymbol{\pi}_j \middle| \Psi[J=1,M_J=0] \right\rangle = -\hat{\mathbf{i}}_z \hbar \sqrt{\frac{v_{nuc}}{v_{mol}}} e^{-G} \sqrt{\frac{3}{4\pi}} \int d^3\mathbf{r} \int d^3\mathbf{r}_a \int d^3\mathbf{r}_b$$
$$\left\{ \Phi_S(\mathbf{r},\mathbf{r}_a,\mathbf{r}_b) \phi_d(|\mathbf{r}_a|) \phi_d(|\mathbf{r}_b|) \left[\left(2F_{DD}(|\mathbf{r}|) + \frac{2}{3} r F'_{DD}(|\mathbf{r}|) \right) \right] \right\} \tag{52}$$

5.4. Specification of Spatial Integrals I and K

It will be convenient to define spatial integrals according to

$$I = \int d^3\mathbf{r} \int d^3\mathbf{r}_a \int d^3\mathbf{r}_b \left\{ \Phi_S(\mathbf{r},\mathbf{r}_a,\mathbf{r}_b) \phi_d(|\mathbf{r}_a|) \phi_d(|\mathbf{r}_b|) F_{DD}(|\mathbf{r}|) \right\}$$

$$K = \int d^3\mathbf{r} \int d^3\mathbf{r}_a \int d^3\mathbf{r}_b \left\{ \Phi_S(\mathbf{r},\mathbf{r}_a,\mathbf{r}_b) \phi_d(|\mathbf{r}_a|) \phi_d(|\mathbf{r}_b|) r F'_{DD}(|\mathbf{r}|) \right\} \tag{53}$$

which we will evaluate numerically. The matrix element in terms of these integrals is

$$\left\langle \Psi[^4\mathrm{He}] \middle| \sum_j \boldsymbol{\sigma}_j \times \boldsymbol{\pi}_j \middle| \Psi[J=1,M_J=0] \right\rangle = -\hat{\mathbf{i}}_z \hbar \sqrt{\frac{v_{nuc}}{v_{mol}}} e^{-G} \sqrt{\frac{3}{4\pi}} \left(2I + \frac{2}{3} K \right) \tag{54}$$

6. Numerical Calculation

Since the model under consideration is simple, we do not expect that it will provide a precise estimate for the **a** matrix element. Consequently, there is little motivation to obtain high precision, which makes the numerical issues much simpler. We have developed a computer program which implements a simple numerical integration, and we are able to get reasonable accuracy without difficulty.

6.1. I Integral

We first expand out the I integral (for clarity) including integration limits

$$I = N_S 8\pi^2 \int_0^{r_{max}} r^2 dr \int_{r_0}^{r_{max}} r_a^2 dr_a \int_0^{\pi} \sin\theta_a d\theta_a \int_{r_0}^{r_{max}} r_b^2 dr_b \int_0^{\pi} \sin\theta_b d\theta_b \int_0^{2\pi} d\phi_b$$
$$\Bigg\{ \phi_d(r_a)\phi_d(r_b) F_{DD}(r) u(r_a) u(r_b)$$
$$u\Bigg(\sqrt{r^2 + \frac{r_a^2}{4} + \frac{r_b^2}{4} + r r_a \cos(\theta_a) + r r_b \cos(\theta_b) + \frac{r_a r_b}{2}\Bigg(\cos(\theta_a)\cos(\theta_b) + \sin(\theta_a)\sin(\theta_b)\cos(\phi_b)\Bigg)}\Bigg)$$
$$u\Bigg(\sqrt{r^2 + \frac{r_a^2}{4} + \frac{r_b^2}{4} + r r_a \cos(\theta_a) - r r_b \cos(\theta_b) - \frac{r_a r_b}{2}\Bigg(\cos(\theta_a)\cos(\theta_b) + \sin(\theta_a)\sin(\theta_b)\cos(\phi_b)\Bigg)}\Bigg)$$
$$u\Bigg(\sqrt{r^2 + \frac{r_a^2}{4} + \frac{r_b^2}{4} - r r_a \cos(\theta_a) + r r_b \cos(\theta_b) - \frac{r_a r_b}{2}\Bigg(\cos(\theta_a)\cos(\theta_b) + \sin(\theta_a)\sin(\theta_b)\cos(\phi_b)\Bigg)}\Bigg)$$
$$u\Bigg(\sqrt{r^2 + \frac{r_a^2}{4} + \frac{r_b^2}{4} - r r_a \cos(\theta_a) - r r_b \cos(\theta_b) + \frac{r_a r_b}{2}\Bigg(\cos(\theta_a)\cos(\theta_b) + \sin(\theta_a)\sin(\theta_b)\cos(\phi_b)\Bigg)}\Bigg)\Bigg\} \quad (55)$$

The K integral is very similar, with

$$F_{DD}(r) \;\rightarrow\; r F'_{DD}(r) \quad (56)$$

6.2. Gaussian Quadrature for θ_a and θ_b

We used Gaussian quadrature for θ_a and for θ_b, with

$$\int_0^{\pi} \sin\theta f(\cos\theta) d\theta = \int_{-1}^{+1} f(x) dx \;\rightarrow\; \sum_j w_j f(x_j) \quad (57)$$

Reasonable accuracy is obtained for this integral with 6 nodes and weights.

6.3. Radial and Angular Integrations

For the radial integrations we used a simple quadrature based on

$$\int_{r_{min}}^{r_{max}} f(r) dr = h_r \sum_j f(r_j) \quad (58)$$

Reasonable accuracy is obtained with on the order of 50 points. It was sufficient to integrate out to

$$r_{max} = 8 \text{ fm} \tag{59}$$

A similar approach was used for the ϕ_b integration

$$\int_0^{2\pi} f(\phi) d\phi = h_\phi \sum_j f(\phi_j) \tag{60}$$

We set the number of nodes for this angular integration to be the same as for the radial integrals.

6.4. Numerical Results

We carried out a set of numerical calculations based on

$$N_a = N_b = N_{\phi_b} = N \tag{61}$$

with the following results

N	N_G	$\sqrt{\langle \lvert\mathbf{r}_4\rvert^2 \rangle}$ fm	$\sqrt{\langle \lvert\mathbf{r}_a\rvert^2 \rangle}$ fm	I fm^{-1}	K fm^{-1}	$I + K/3$ fm^{-1}
30	6	1.44797	2.36425	−72.8664	53.3381	−55.0871
40	6	1.44792	2.36414	−72.8622	53.3344	−55.0840
50	6	1.44791	2.36411	−72.8602	53.3328	−55.0826
60	6	1.44790	2.36409	−72.8593	53.3321	−55.0819
30	8	1.44793	2.36419	−72.8683	53.3348	−55.0901
40	8	1.44788	2.36409	−72.8642	53.3311	−55.0872
50	8	1.44787	2.36405	−72.8622	53.3295	−55.0857
60	8	1.44786	2.36403	−72.8614	53.3288	−55.0851
70	10	1.44787	2.36405	−72.8621	53.3298	−55.0854
80	10	1.44787	2.36405	−72.8618	53.3296	−55.0852

The results do not change much with different numbers of grid points or number of Gaussian nodes.

6.5. Magnitude of the $\mathbf{a}$-Matrix Element

We start by developing an estimate for the $\boldsymbol{\sigma} \times \boldsymbol{\pi}$ matrix element, which is

$$\left| \left\langle \Psi[^4\text{He}] \right| \sum_j \boldsymbol{\sigma}_j \times \boldsymbol{\pi}_j \left| \Psi[J=1, M_J=0] \right\rangle \right| = \hbar \sqrt{\frac{3}{4\pi}} \left| 2I + \frac{2}{3} K \right| \sqrt{\frac{v_{nuc}}{v_{mol}}} e^{-G}$$

$$= 53.83 \, \hbar \sqrt{\frac{v_{nuc}}{v_{mol}}} e^{-G} \tag{62}$$

The magnitude of the $\mathbf{a}$ matrix element from the model is

$$|\langle \Psi[^4\text{He}] | \mathbf{a} | \Psi[J=1, M_J=0] \rangle| = \frac{\Delta M c^2}{2 M_{4He} c^2} \left| \left\langle \Psi[^4\text{He}] \right| \sum_j \boldsymbol{\sigma}_j \times \frac{\boldsymbol{\pi}_j}{mc} \left| \Psi[J=1, M_J=0] \right\rangle \right|$$

$$= 0.0362 \sqrt{\frac{v_{nuc}}{v_{mol}}} e^{-G} \tag{63}$$

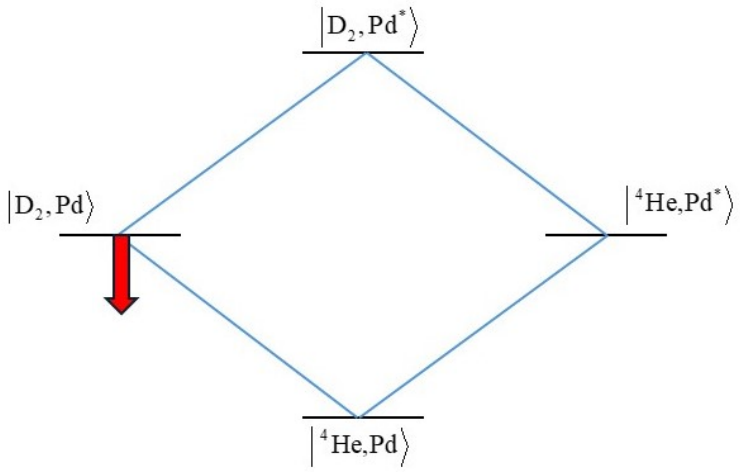

Figure 4. Basic diamond schematic for excitation transfer. The molecular D_2 in the initial state can decay by 3+1 fusion; however, the D_2 in the off-resonant state at the top of the diamond is in energy deficit relative to the energy eigenvalue, and the 3+1 decay channel is not open.

7. Impact of Loss on the a-Matrix Element

In 2002 we proposed that off-resonant loss could make a big difference in the rate for energy exchange via multi-quantum exchange. The scheme under consideration was one in which indirect excitation transfer involving exchange with an oscillator would result in intermediate levels off of resonance, where it would be expected that loss channels that are open in one pathway would not be open in the other pathway. According to our interpretation, it would be the oscillator that would be off of resonance under these conditions, so that in one pathway the oscillator would be able to drive loss channels while in the other it would not. It was proposed that this would reduce the destructive interference, and greatly enhance the indirect coupling responsible for excitation transfer.

We recently understood that there was an issue with the model in the way that we were working with it. According to the new understanding, it is true that the scheme would impact the destructive interference, and it is true that the oscillator could be viewed as being off of resonance; however, it is not the case that the loss rate associated with the oscillator coupling is fast (as we had proposed). The problem was that we did not include the destructive interference associated with the different pathways that contribute to the loss. If this destructive interference is not included, then the rate of off-resonant loss is extremely fast (as concluded in our many earlier papers); however, if the destructive interference is included, it eliminates all contributions not directly involved in the excitation transfer process. The conclusion is that the effect proposed is certainly a real effect, and it certainly contributions to a reduction of the destructive interference involved in excitation transfer; however, the magnitude of the effect is very small.

The conclusion is that if we would like for off-resonant loss to impact excitation transfer, we need for the off-resonant loss effects to be directly associated with the states involved in the excitation transfer process. One example of this is in the $D_2/^4He$ transition, where the D_2 state has a fusion loss channel where 3+1 fusion products (p+t and n+^{3}He) can be produced. This decay channel is open in the initial state, but is not open in the intermediate states (see Figure 4). In this kind of scheme, the loss channel works differently between the two pathways, so we would expect the destructive interference between the two pathways to be reduced. At issue is how to include this effect in a model.

7.1. Imaginary Potential Model

In nuclear physics models, loss processes are sometimes taken into account through the use of an imaginary potential. In the case of D_2 scattering, people have included the effect of loss to 3+1 fusion channels through the use of an imaginary potential according to

$$V(r) \;\rightarrow\; V(r) + iW(r) \tag{64}$$

where $W(r)$ is the imaginary potential. To model the impact of loss of deuteron-deuteron scattering, Chwieroth et al (1972) [24] made use of an imaginary potential of the form

$$W(r) = -W_0 \left(\frac{1}{1+e^{(r-R_0)/a}} + \frac{4e^{(r-R_0)/a}}{(1+e^{(r-R_0)/a})^2} \right) \tag{65}$$

and give parameters for the ^{3}P channel for scattering at 12.65 MeV. This model was also used by Kurihara (1985) [25] to model deuteron-deuteron scattering. We would not expect the parameters used at these energies to be relevant to loss in molecular D_2. For our model we have kept the shape (as modeled with the R_0 and a parameters), but we adjusted the depth of the imaginary potential in order to match the loss from the ^{4}He $T = 0$ $J^\pi = 1^-$ d+d excited state at 28.37 MeV given by Tilley et al [26]. The model parameters are

$$\begin{aligned} W_0 &= 0.066 \text{ MeV} \\ R_0 &= 3.75 \text{ fm} \\ a &= 0.5 \text{ fm} \end{aligned} \tag{66}$$

7.2. Spatial Integrals with Loss

For $N = 40$ and $N_\phi = 6$ we get

$$\begin{aligned} I &= -72.8461 - i0.823198 \\ K &= 53.3265 + i0.289773 \\ I + \frac{1}{3}K &= -55.0706 - i0.726607 \end{aligned} \tag{67}$$

7.3. Parameterization of the Difference

What is important in this kind of model is the magnitude of the relative difference between the **a**-matrix elements. We can write the the matrix element calculated with loss in terms of the matrix element without loss as

$$\langle \Psi[^4\text{He}] | \mathbf{a} | \Psi[J=1, M_J=0] \rangle_{with\ loss} = \eta \langle \Psi[^4\text{He}] | \mathbf{a} | \Psi[J=1, M_J=0] \rangle_{no\ loss} \tag{68}$$

where

$$\eta = 0.999757 + i0.0131909 \tag{69}$$

We can evaluate the magnitude of the difference to be

$$|1 - \eta| = 0.0132 \tag{70}$$

8. Discussion and Conclusions

We have recently proposed new schemes intended to model excess heat, transmutation, and low-level energetic nuclear emission in LENR experiments with PdD_x, which are based on coherent dynamics involving the D_2/^{4}He transition, and also involving transitions to highly excited nuclear molecule states based on clusters. A key parameter needed to quantify the new models is the matrix element for the relativistic phonon-nuclear $\mathbf{a} \cdot c\mathbf{P}$ interaction, which has in part motivated this work.

In the model under discussion in this paper, we evaluated the $\mathbf{a}$ matrix element by brute force using Mathematica. For the ^{4}He nucleus, we made use of a relatively simple spatial wave function composed of products of simple functions of the different $|\mathbf{r}_{jk}|$ to account for the dominant S-state component. For the molecular D_2 ^{3}P wave function, we used a spatial wave function composed of products of deuteron wave functions for $|\mathbf{r}_{21}|$ and $|\mathbf{r}_{43}|$, multiplied by the D_2 molecular wave function. When augmented with spin and isospin wave functions and properly symmetrized, we end up with a basic approximate description of the initial and final states. The construction in both cases is completely straightforward, although in the end the overall molecular wave function involves many terms.

We used a brute force Mathematica calculation to evaluate the spin and isospin components of the matrix elements. This leads to reduced matrix elements that involve integrations over functions of space, which we are able to evaluate numerically without difficulty. The overall calculation seems to be a good way to develop an estimate for the $\mathbf{a}$-matrix element, one which sheds light on the various issues that come up in the calculation.

Based on the calculations described above, the three non-zero matrix elements for this model are

$$\langle \Psi[^4\mathrm{He}]|\mathbf{a}|\Psi[J=1,M_J=+1]\rangle = -\left(\frac{\hat{\mathbf{i}}_x + i\hat{\mathbf{i}}_y}{\sqrt{2}}\right) 0.0362 \sqrt{\frac{v_{nuc}}{v_{mol}}} e^{-G} \tag{71}$$

$$\langle \Psi[^4\mathrm{He}]|\mathbf{a}|\Psi[J=1,M_J=0]\rangle = \hat{\mathbf{i}}_z \, 0.0362 \sqrt{\frac{v_{nuc}}{v_{mol}}} e^{-G} \tag{72}$$

$$\langle \Psi[^4\mathrm{He}]|\mathbf{a}|\Psi[J=1,M_J=-1]\rangle = \left(\frac{\hat{\mathbf{i}}_x - i\hat{\mathbf{i}}_y}{\sqrt{2}}\right) 0.0362 \sqrt{\frac{v_{nuc}}{v_{mol}}} e^{-G} \tag{73}$$

with

$$\sqrt{\frac{v_{nuc}}{v_{mol}}} = 6.64 \times 10^{-12} \tag{74}$$

and with

$$G = 90.35 \tag{75}$$

Since the model is so simple, we are able to evaluate the numerical matrix element accurately, and quote three significant digits for the matrix elements that result. However, since the model is so simple, it leaves out a number of important effects which contribute. Nucleons from one deuteron can get arbitrarily close to nucleons in the other deuteron in this model, but not a more sophisticated model. We have accounted for the ^{1}S configuration for the alpha particle, but not for the other configurations that contribute to the overall wave function. And we have included the ^{3}S configuration for the deuteron, but not the ^{1}D. The conclusion is that we expect significant corrections to the simple model result when more accurate nuclear models are used.

Appendix A. Relative Strength of the $-\mathbf{d} \cdot \mathbf{E}$ and $\mathbf{a} \cdot c\mathbf{P}$ Interactions

Electric dipole transitions are expected to be stronger than magnetic dipole, electric quadrupole, or electric or magnetic transitions of higher multipolarity. It is true that our motivation for considering the relativistic phonon-nuclear inter-

action was to find stronger coupling than what could be obtained from electric dipole interactions. What is of interest then is to quantify how strong the two different interactions are under identical conditions.

We are interested in developing an estimate for the ratio

$$\rho = \frac{|\langle \Psi_f | \mathbf{a} \cdot c\mathbf{P} | \Psi_i \rangle|}{|\langle \Psi'_f | - \mathbf{d} \cdot \mathbf{E} | \Psi'_i \rangle|} \sim \frac{|\langle \Psi_f | \mathbf{a} | \Psi_i \rangle|}{|\langle \Psi'_f | \mathbf{d} | \Psi'_i \rangle|} \frac{c|\mathbf{P}|}{|\mathbf{E}|} \tag{A.1}$$

for transitions that are roughly matched, under conditions where the vibrational excitation is the same.

Appendix A.1. Estimate for the Ratio of $\mathbf{E}$ and $\mathbf{P}$

Under the assumption that the nuclear system is accelerated by the local electric field, and it is that electric field which mediates transitions, then the center of mass momentum is driven by the electric field according to Newton's law

$$\frac{d}{dt}\mathbf{P} = q\mathbf{E} \tag{A.2}$$

In this case the magnitude of the electric divided by the momentum is

$$\frac{|\mathbf{E}|}{|\mathbf{P}|} = \frac{\omega}{q} \tag{A.3}$$

where ω is the frequency of the vibrations. The electric field and momentum are out of phase, but that is not important for the estimate of the ratio of the matrix elements we are interested in.

Appendix A.2. Estimate for the Electric Dipole Transition Matrix Element

For the electric dipole (E1) transition moment we can estimate

$$|\langle \Psi'_f | \mathbf{d} | \Psi'_i \rangle| \sim O(E1)\, e\,\text{fm} \tag{A.4}$$

where we consider an electric dipole moment on the general order of e-fm to correspond to a transition with unit transition strength, and where $O(E1)$ is the square root of the normalized E1 transition strength.

Appendix A.3. Estimate for the $\mathbf{a}$-Matrix Element

We can think of the relativistic phonon nuclear interaction according to

$$\hat{H}_{int} = \frac{1}{2Mc} \sum_{j<k} \left[\beta_j \boldsymbol{\alpha}_j + \beta_k \boldsymbol{\alpha}_k, \hat{V}_{jk} \right] \cdot c\mathbf{P} \rightarrow \mathbf{a} \cdot c\mathbf{P} \tag{A.5}$$

which can be used to define the $\mathbf{a}$ operator

$$\mathbf{a} = \frac{1}{2Mc^2} \sum_{j<k} \left[\beta_j \boldsymbol{\alpha}_j + \beta_k \boldsymbol{\alpha}_k, \hat{V}_{jk} \right] \tag{A.6}$$

If we make use of the identity discussed briefly in the introduction, then we can take the matrix element of the $\mathbf{a}$ operator to be

$$|\langle \Psi_f | \mathbf{a} | \Psi_i \rangle| = \left| \left\langle \Psi_f \left| \frac{1}{2i} \frac{\Delta E}{Mc^2} \left(\sum_j \boldsymbol{\sigma}_j \times \frac{\boldsymbol{\pi}_j}{mc} \right) \right| \Psi_i \right\rangle \right| \sim \frac{1}{2} \frac{\Delta E}{Mc^2} \left(\frac{O(M2)\, \hbar\, (1\,\text{fm}^{-1})}{mc} \right) \tag{A.7}$$

Appendix A.4. Estimate for the Ratio

We can use these rough estimates to write

$$\rho \sim \frac{\frac{1}{2}\frac{\Delta E}{Mc^2}\left(\frac{O(M2)\ \hbar\ (1\ \mathrm{fm}^{-1})}{mc}\right)}{O(E1)\ e\ \mathrm{fm}}\frac{Zec}{\omega} \tag{A.8}$$

We can work on this and write

$$\rho \sim \frac{Z}{2}\frac{O(M2)}{O(E1)}\frac{\Delta E}{Mc^2}\frac{\hbar\,(1\ \mathrm{fm}^{-1})}{mc}\frac{c}{\omega\ (1\ \mathrm{fm})} \tag{A.9}$$

We can evaluate

$$\frac{\hbar\,(1\ \mathrm{fm}^{-1})}{mc} = 0.210164 \tag{A.10}$$

$$\frac{c}{\omega\ (1\ \mathrm{fm})} = 4.77135\times 10^{16}\left(\frac{1\ \mathrm{MHz}}{f_A}\right) \tag{A.11}$$

We can use these to write

$$\begin{aligned}\rho &\sim 5.01\times 10^{15}\ Z\left(\frac{O(M2)}{O(E1)}\right)\left(\frac{\Delta E}{Mc^2}\right)\left(\frac{1\ \mathrm{MHz}}{f_A}\right)\\ &= 5.38\times 10^{6}\ \frac{Z}{A}\left(\frac{O(M2)}{O(E1)}\right)\left(\frac{\Delta E}{1\ \mathrm{MeV}}\right)\left(\frac{1\ \mathrm{MHz}}{f_A}\right)\end{aligned} \tag{A.12}$$

Appendix A.5. Conclusion

Based on these estimates, we conclude that the relativistic phonon-nuclear $\mathbf{a}\cdot c\mathbf{P}$ interaction is much stronger than the electric dipole $-\mathbf{d}\cdot\mathbf{E}$ interaction for interactions of high-energy nuclear transitions with a highly-excited phonon mode.

Appendix B. The $\boldsymbol{\sigma}\times\mathbf{p}$ Operator is a Tensor Operator

For an operator to be a tensor operator, it must transform under a rotation according to [27]

$$T_q^{(k)} = \sum_{q'} T_{q'}^{(k)} D_{q,q'}^{(k)}(\alpha,\beta,\gamma) \tag{B.1}$$

In this expression $T_q^{(k)}$ is a component of a tensor operator of rank k, where $D_{q,q'}^{(k)}(\alpha,\beta,\gamma)$ is the Wigner D-function, and where α,β,γ are Euler angles. In the case of an incremental rotation, this is consistent with

$$[J_\pm, T_q^{(k)}] = \hbar\sqrt{(k\mp q)(k\pm q+1)}\,T_{q\pm 1}^{(k)} \tag{B.2}$$

where $\mathbf{J}$ is the total angular momentum operator, and where $J_\pm$ are the associated raising and lowering operators. Of interest here is to see whether tensor operators consistent with the $\boldsymbol{\sigma}\times\mathbf{p}$ operator can be constructed that satisfy this relation.

Appendix B.1. Particle Momentum Variables

The $\boldsymbol{\sigma}\times\boldsymbol{\pi}$ interaction is written in terms of $\boldsymbol{\pi}$, which is the nucleon momentum for the relative problem after separation from the center of mass degrees of freedom. The momentum of the particle as an independent particle is $\mathbf{p}$. By focusing on the $\boldsymbol{\sigma}\times\mathbf{p}$ interaction (instead of the $\boldsymbol{\sigma}\times\boldsymbol{\pi}$ interaction), the arguments and calculation are a bit simpler. For a nucleus at rest the two momentum operators are the same. Ultimately, we are interested in the calculation of matrix elements for nuclear wave functions that are in the rest frame.

Appendix B.2. Cartesian Components and $T_0^{(1)}$

We can evaluate the $\boldsymbol{\sigma}\times\mathbf{p}$ operator and write

$$\boldsymbol{\sigma}\times\mathbf{p} = \begin{vmatrix} \hat{\mathbf{i}}_x & \hat{\mathbf{i}}_y & \hat{\mathbf{i}}_z \\ \sigma_x & \sigma_y & \sigma_z \\ p_x & p_y & p_z \end{vmatrix} = \hat{\mathbf{i}}_x(\sigma_y p_z - \sigma_z p_y) + \hat{\mathbf{i}}_y(\sigma_z p_x - \sigma_x p_z) + \hat{\mathbf{i}}_z(\sigma_x p_y - \sigma_y p_x) \tag{B.3}$$

Since the cross product is a vector, we expect that the corresponding tensor operator will be a rank 1 operator. We also expect that the $q=0$ component will be the z-component of the $\boldsymbol{\sigma}\times\mathbf{p}$ operator, so we will assert that

$$T_0^{(1)} = \sigma_x p_y - \sigma_y p_x \tag{B.4}$$

Appendix B.3. Raising and Lowering Operators

We recall that the total angular momentum for a spin 1/2 particle is

$$\mathbf{J} = \mathbf{L} + \mathbf{s} \tag{B.5}$$

where $\mathbf{L}$ is the orbital angular momentum operator and where $\mathbf{s}$ is the spin operator. Consequently, it follows that

$$[J_\pm, T_0^{(1)}] = [L_\pm, T_0^{(1)}] + [s_\pm, T_0^{(1)}] \tag{B.6}$$

The individual raising and lowering operators are

$$L_\pm = L_x \pm iL_y = (yp_z - zp_y) \pm i(zp_x - xp_z) s_\pm = s_x \pm is_y = \frac{\hbar}{2}(\sigma_x \pm i\sigma_y) \tag{B.7}$$

Appendix B.4. Evaluation of $[J_+, T_0^{(1)}]$

For the commutator with the raising operator, we first evaluate the spin contribution and write

$$\begin{aligned} [s_+, T_0^{(1)}] &= \frac{1}{2}\hbar[\sigma_x + i\sigma_y, \sigma_x p_y - \sigma_y p_x] \\ &= -\frac{1}{2}\hbar[\sigma_x, \sigma_y]p_x + i\frac{1}{2}\hbar[\sigma_y, \sigma_x]p_y \\ &= -i\hbar\sigma_z p_x + \hbar\sigma_z p_y \\ &= -i\hbar\sigma_z(p_x + ip_y) \end{aligned} \tag{B.8}$$

For the contribution from the angular momentum raising operator we have

$$[L_+, T_0^{(1)}] = \Big[yp_z - zp_y + izp_x - ixp_z, \sigma_x p_y - \sigma_y p_x\Big]$$

$$
\begin{aligned}
&= ip_z[x,p_x]\sigma_y + p_z[y,p_y]\sigma_x \\
&= -\hbar p_z\sigma_y + i\hbar p_z\sigma_x \\
&= i\hbar p_z(\sigma_x + i\sigma_y)
\end{aligned} \tag{B.9}
$$

This leads to

$$
[J_+, T_0^{(1)}] = -i\hbar\sigma_z(p_x + ip_y) + i\hbar p_z(\sigma_x + i\sigma_y) \tag{B.10}
$$

This we compare with

$$
[J_+, T_0^{(1)}] = \sqrt{2}\hbar T_1^{(1)} \tag{B.11}
$$

with the result that

$$
T_1^{(1)} = -i\sigma_z\frac{p_x + ip_y}{\sqrt{2}} + ip_z\frac{\sigma_x + i\sigma_y}{\sqrt{2}} \tag{B.12}
$$

Appendix B.5. Evaluation of $[J_-, T_0^{(1)}]$

For the other case, we start with the spin contribution to the commutator and write

$$
\begin{aligned}
[s_-, T_0^{(1)}] &= \frac{1}{2}\hbar[\sigma_x - i\sigma_y, \sigma_x p_y - \sigma_y p_x] \\
&= -\frac{1}{2}\hbar[\sigma_x,\sigma_y]p_x - i\frac{1}{2}\hbar[\sigma_y,\sigma_x]p_y \\
&= -i\hbar\sigma_z p_x - \hbar\sigma_z p_y \\
&= -i\hbar\sigma_z(p_x - ip_y)
\end{aligned} \tag{B.13}
$$

For the angular momentum contribution to the commutator we have

$$
\begin{aligned}
&\left[L_x - iL_y, \sigma_x p_y - \sigma_y p_x\right] \\
&= \left[yp_z - zp_y - izp_x + ixp_z, \sigma_x p_y - \sigma_y p_x\right] \\
&= -ip_z[x,p_x]\sigma_y + p_z[y,p_y]\sigma_x \\
&= +\hbar p_z\sigma_y + i\hbar p_z\sigma_x \\
&= i\hbar p_z(\sigma_x - i\sigma_y)
\end{aligned} \tag{B.14}
$$

This leads to

$$
[J_-, T_0^{(1)}] = -i\hbar\sigma_z(p_x - ip_y) + i\hbar p_z(\sigma_x - i\sigma_y) \tag{B.15}
$$

This we compare with

$$
[J_-, T_0^{(1)}] = \sqrt{2}\hbar T_{-1}^{(1)} \tag{B.16}
$$

with the result that

$$
T_{-1}^{(1)} = -i\sigma_z\frac{p_x - ip_y}{\sqrt{2}} + ip_z\frac{\sigma_x - i\sigma_y}{\sqrt{2}} \tag{B.17}
$$

Appendix B.6. Tensor Operator in Terms of $\boldsymbol{\sigma} \times \mathbf{p}$ Components

We can make use of these results and identify them with the Cartesian components of the $\boldsymbol{\sigma} \times \mathbf{p}$ operator. This leads to

$$T_1^{(1)} = -\frac{\Big(\boldsymbol{\sigma} \times \mathbf{p}\Big)_x + i\Big(\boldsymbol{\sigma} \times \mathbf{p}\Big)_y}{\sqrt{2}} \tag{B.18}$$

$$T_0^{(1)} = \Big(\boldsymbol{\sigma} \times \mathbf{p}\Big)_z \tag{B.19}$$

$$T_{-1}^{(1)} = \frac{\Big(\boldsymbol{\sigma} \times \mathbf{p}\Big)_x - i\Big(\boldsymbol{\sigma} \times \mathbf{p}\Big)_y}{\sqrt{2}} \tag{B.20}$$

For reference, we recall that the spherical harmonics (which are tensor operators) are related to the Cartesian components of the positive vector according to

$$\begin{aligned} rY_{1,1} &= -\sqrt{\frac{3}{4\pi}}\frac{x+iy}{\sqrt{2}} \\ rY_{1,0} &= \sqrt{\frac{3}{4\pi}}z \\ rY_{1,-1} &= \sqrt{\frac{3}{4\pi}}\frac{x-iy}{\sqrt{2}} \end{aligned} \tag{B.21}$$

Appendix B.7. Conclusion

We see that the construction is straightforward, and we conclude that the $\boldsymbol{\sigma} \times \mathbf{p}$ operator is a tensor operator.

References

[1] P. L. Hagelstein and I. U. Chaudhary, "Including Nuclear Degrees of Freedom in a Lattice Hamiltonian," *J Condensed Matter Nuclear Science* **7** (2012) 35–50.

[2] G. Breit, "Approximately Relativistic Equations," *Phys. Rev.* **53** (1938) 153–173.

[3] M. Järvinen, "Hydrogen atom in relativistic motion," *Phys. Rev. D* **71** (2005) 085006.

[4] P. L. Hagelstein and I. U. Chaudhary, "Central and Tensor Contributions to the Phonon-exchange Matrix Element for the $D_2/^4$He Transition," *J Condensed Matter Nuclear Science* **11** (2013) 15-58.

[5] P. L. Hagelstein, "Quantum Composites: A Review, and New Results for Models for Condensed Matter Nuclear Science," *J Condensed Matter Nuclear Science* **20** (2016) 139–225.

[6] P. L. Hagelstein, "Nonrelativistic Reduction of the Phonon-nuclear Interaction for the One-pion Exchange Potential with Pseudovector Interaction," *J Condensed Matter Nuclear Science* **34** (2021) 101–109.

[7] P. L. Hagelstein, "Reduction of the HD/^{3}He Phonon-Nuclear Matrix Element," *J Condensed Matter Nuclear Science* **34** (2021) 110–131.

[8] P. L. Hagelstein, "Lowest-order relativistic interaction between lattice vibrations and internal degrees of freedom of a nucleus," *J. Phys. B: Atomic, Molecular and Optical Physics* **56** (2023) 195002.

[9] M. Gell-Mann, "Isotopic Spin and New Unstable Particles," *Phys. Rev.* **92** (1953) 833–834.

[10] H. C. Urey and D. Rittenberg, "Some Thermodynamic Properties of the H^1H^2, H^2H^2 Molecules and Compounds Containing the H^2 Atom, *J. Chem. Phys.* **1** (1933) 137.

[11] J. L. Langenbrunner, G. Feldman, H. R. Weller, D. R. Tilley, B. Wachter, T. Mertelmeier, and H. M. Hofmann, "^{2}H(d,γ)He reaction at E_d=1.2 MeV," *Phys. Rev. C* **38** (1988) 565–568.
[12] D. V. Balin, V. A. Ganzha, S. M. Kozlov, E. M. Maev, G. E. Petrov, M. A. Soroka, G. N. Schapkin, G. G. Semenchuk, V. A. Trofimov, A. A. Vasiliev, A. A. Vorobyov, N. I. Voropaev, C. Petitjean, B. Gartner, B. Lauss, J. Marton, J. Zmeskal, T. Case, K. M. Crowe, P. Kammel, F. J. Hartmann and M. P. Faifman, "High Precision Study of Muon Catalyzed Fusion in D_2 and HD Gas," *Physics of Particles and Nuclei* **42** (2011) 185–214.
[13] G. M. Hale, "Nuclear physics of the muon catalyzed d+d reactions," *Muon Catalyzed Fusion*, edited by L. I. Ponomarov and C. Petitjean, J. C. Balzer Publishing Co. Basel (1990) 227–232.
[14] H. Kamada, A. Nogga, W. Gloeckle, E. Hiyama, M. Kamimura, K. Varga, Y. Suzuki, M. Viviani, A. Kievsky, S Rosati and J, Carlson, "Benchmark test calculation of a four-nucleon bound state," *Physical Review C* **64** (2001) 044001.
[15] I. U. Chaudhary, *Applications of Group Theory to Few-Body Physics*, PhD Thesis, MIT (2005).
[16] J. Carlson, *Phys. Rev. C* **38** (1988) 1879.
[17] Z. Xuan and Z. Fan-An, "Soft repulsive core effects in (d+d) scattering and reaction," *Nuclear science and Engineering* **89** (1985) 351–361.
[18] E. Epelbaum, W. Glöckle and U. G. Meissner, "The two-nucleon system at next-to-next-to-next-to-leading order," *Nuclear Physics A* **747** (2005) 362–424.
[19] E. L. Tomusiak, W. Leidemann and H.M. Hofmann, *Phys. Rev. C* **52** (1995) 1963.
[20] A. A. Frost and B. Musulin, *J. Chem. Phys.* **22** (1954) 1017.
[21] W. Kolos and L. Wolniewicz, "Improved theoretical ground-state energy of the hydrogen molecule," *The Journal of Chemical Physics* **49** 404–410.
[22] L. Cohen, "Classification of alpha particle wave functions," *Nuclear Physics* **20** (1960) 690–697.
[23] J. E. Beam, "Orthogonal classification of alpha-particle wave functions," *Physical Review* **158** (1967) 907.
[24] F. S. Chwieroth, Y. C. Tang and D. R. Thompson, "Study of d+d scattering with the resonating-group method and an imaginary potential," *Nuclear Physics A* **189** (1972) 1–19.
[25] Y. Kurihara, "Nuclear collision theory with many-body correlations. II: Deuteron+deuteron elastic scattering," *Progress of Theoretical Physics* **73** (1985) 1471–1484.
[26] D. R. Tilley, H. R. Weller and G. M. Hale, "Energy levels of light nuclei $A = 4$," *Nuclear Physics A* **541** (1992) 1–104.
[27] D. A. Varshalovich, A. N. Moskalev and V. K. Khersonskii, *Quantum Theory of Angular Momentum*, World Scientific, New Jersey (2015).